MAAP5 APPLICATION TO IN-VESSEL RETENTION ANALYSIS FOR PRESSURIZED LIGHT WATER REACTORS

Paul McMinn[1], Chan Y. Paik[1], and Quan Zhou[1]

[1] *Fauske & Associates, LLC: 16W07083rd Street, Burr Ridge, Illinois, 60527,*
mcminn@fauske.com, paik@fauske.com, zhou@fauske.com

This paper describes the application of the Modular Accident Analysis Program version 5 (MAAP5[a]) computer code to the analysis of the efficacy of severe accident management strategies for the prevention of vessel failure in Pressurized Light Water Reactors (PWRs).[1] A method is described for the calculation of the probability of vessel failure as a function of operator action delay time. The method includes consideration of uncertainties using a Monte Carlo approach for the calculation of probabilities. Sample results are calculated and presented for two In-Vessel Retention (IVR) strategies, in-vessel injection (IVI) and external reactor vessel cooling (ERVC). The sample calculations are performed for severe accidents occurring both at full power and shutdown operating conditions for a plant with lower head penetrations. Results show that IVI is an effective IVR strategy for accidents occurring both at full power and during shutdown conditions while ERVC is only an effective IVR strategy for accidents occurring during shutdown conditions. This is mainly because of the weakness of the lower head penetrations when the lower head wall is thermally attacked by molten corium. The combination of IVI and ERVC is only marginally more effective than IVI alone.

I. INTRODUCTION

Severe accidents in pressurized light water reactors can occur due to inadequate heat removal brought about by either a loss of coolant or a loss of sufficient heat removal capacity (such as an extended loss of power event). In these conditions, the fuel in the reactor core will heat up and melt. This process alters the geometry of the reactor core, changing it from a coolable geometry to a potentially non-coolable geometry. If the melt progression is not arrested, the core material will slump into the reactor vessel lower head and challenge the structural integrity of the reactor vessel lower head wall. If the reactor vessel fails, molten core debris will relocate into the reactor vessel cavity where it can release additional fission products and challenge containment integrity due to molten-core-concrete interaction.

In-vessel retention of core material is a key goal of severe accident management strategies. In order to achieve this goal, lower head failure must be prevented either by stabilization of the core material within the core boundary or by removing sufficient heat from the debris or vessel wall in the lower plenum to prevent the temperature of the vessel wall from rising to the point where the strength of steel is no longer sufficient to sustain the imposed loads. In-vessel injection is capable of stabilizing the core material in the core, prior to relocation into the lower plenum if injection is initiated early enough. If initiated at a later time, in-vessel injection can remove heat from the debris directly and lower the temperature or ingress into the gap between the debris bed and the lower plenum wall to allow for heat removal from the wall. External reactor vessel cooling is achieved by flooding the reactor vessel cavity such that the water removes decay heat through the reactor vessel wall.

This paper investigates the effectiveness of In-Vessel Injection (IVI) and External Reactor Vessel Cooling (ERVC) as severe accident mitigation strategies. This is done via calculation using the MAAP5 code. The calculation methodology includes a quantification of uncertainty using a Monte Carlo approach in order to capture the full spectrum of plausible code results. These results are then used to evaluate the probability of keeping the reactor vessel intact when employing IVI and ERVC as severe accident mitigation strategies.

II. ACCIDENT SEQUENCES

This analysis investigates severe accidents occurring at full power and during shutdown conditions for a PWR. The reactor design includes instrumentation tube penetrations in the lower head of the reactor vessel, a reliable reactor vessel

---

[a] MAAP is a computer code that is used for integrated severe accident analysis. The MAAP code is owned by the Electric Power Research Institute (EPRI).

depressurization method, and a reactor vessel insulation design that promotes heat transfer to water. The lower head penetrations are of concern because the closure welds (on the inside of the reactor vessel lower head) are susceptible to failure when molten core debris relocates into the reactor vessel lower plenum. The reliable depressurization method is important because it reduces the strain on the reactor vessel lower head during IVR and it allows for the injection of water into the vessel using low pressure pumps (including portable pumps during an extended loss of AC power). The insulation design increases the amount of heat that can be removed from the outside of the reactor vessel lower head when it is submerged in water.

The analyzed initiator for accidents occurring at full power conditions is a small break Loss of Coolant Accident (LOCA) with only the accumulators available prior to core damage. Primary system pressure decreases due to the LOCA and the accumulators inject to keep the core covered for the first several hours. The onset of the severe accident begins between 5 and 8 hours into the sequence (approximately 5 to 8 hours after reactor shutdown) for this initiator. The reactor vessel is fully depressurized after the onset of the accident via the reliable depressurization system. Three strategies are investigated for the mitigation of the severe accident: IVI using an external low pressure pump, flooding of the reactor cavity to achieve ERVC, and simultaneous IVI and reactor cavity flooding. Each of these strategies is implemented at some delay time after the onset of the severe accident.

The analyzed initiator for accidents occurring at shutdown conditions is a loss of shutdown cooling occurring during mid-loop operation (Plant Operating State 5) four days after reactor shutdown. No engineered safeguards are available prior to core damage. This initiator causes rapid heat up and boil-off of the vessel inventory, leading to core damage approximately two hours into the accident (approximately 98 hours after reactor shutdown). The decay power at the onset of the severe accident for this initiator is approximately half of the decay power at the onset of the severe accident for the small break LOCA initiator occurring at full power. Two strategies are investigated for the mitigation of the severe accident: IVI using an external low pressure pump and flooding of the reactor cavity to achieve ERVC. Each of these strategies is implemented at some delay time after the onset of the severe accident.

III. REACTOR VESSEL LOWER PLENUM RESPONSE DURING A SEVERE ACCIDENT

The success of an IVR strategy is dependent on the heat transfer between core debris, metal structure, and water in the reactor vessel lower plenum. These elements interact in complex ways and many factors must be considered in order to achieve accurate calculation of IVR results. The key factors governing the success of IVR are the configuration of the debris in the lower plenum, the possible reactor vessel failure mechanisms, and the available debris cooling mechanisms. These are discussed in the following subsections.

III.A. LOWER PLENUM DEBRIS BED CONFIGURATION

All the sequences investigated in this paper still have a significant pool of water in the reactor vessel lower plenum when molten core material begins relocating from the core into the reactor vessel lower plenum. As the jet of molten core debris enters the water pool, material is stripped off and particulated. This allows for a substantial portion of the core debris to be cooled by the water prior to reaching the reactor vessel lower head wall. The remaining coherent portion of the molten core debris jet will impinge on the lower head wall. If the lower head wall remains intact, the coherent debris jet will form a molten corium pool at the bottom of the reactor vessel lower head which will quickly develop solidified crusts at its boundaries. The particles stripped off during the interaction of the jet and water will eventually settle on top of the corium pool, forming a particle bed, as shown in Figure 1(a).
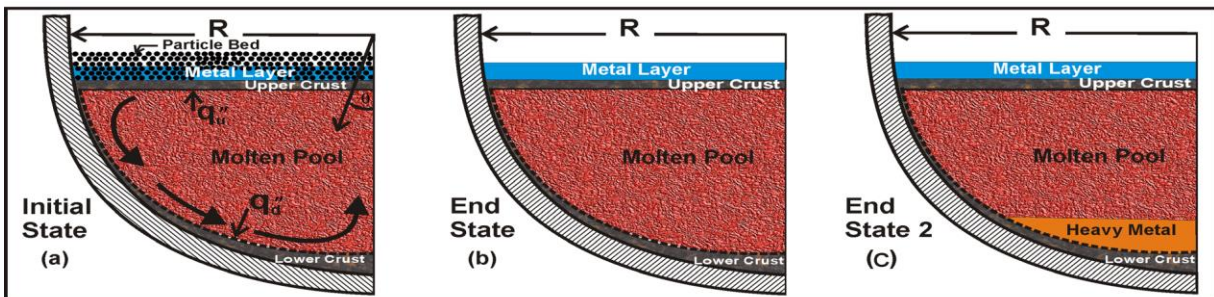

Figure 1, Corium structure in MAAP5.03 : (a) initial state; (b) end state with two-layers; (c) end state with three-layers.

The corium pool in the lower plenum is initially a mixture of metallic and oxidic core debris under a pool of water. As the water boils away and the pool heats up, the metallic portion of the core debris (primarily steel and zirconium metal) will separate from the debris pool, forming a segregated metal layer. The particle bed will melt into the debris pool, achieving a stratified two-layer configuration of light metal over heavier oxidic debris, as shown in Figure 1(b). At high temperature, uranium dioxide can be reduced to elemental uranium by zirconium metal and steel. Uranium metal is more dense than the oxidic debris. After this reaction occurs, the corium pool can achieve a three layer configuration, with a heavy metal layer (primarily elemental uranium, zirconium, steel, and a small amount of oxygen) beneath the oxidic pool, as shown in Figure 1(c).

The MAAP5.03 code is equipped with a heavy metal layer model to assess heavy metal formation. If the temperature in the molten part of oxidic pool is greater than the miscibility gap transition temperature (2,670 K) the chemical reactions forming heavy metal are evaluated in the code. The amount of material that participates in the reaction of heavy metal is assumed as the following:

Material	Amount Available for Heavy Metal Formation
UO_2, ZrO_2	100% of the mass in the lower plenum corium pool
Un-oxidized Zr	A fraction of the un-oxidized Zirconium that is specified via an input parameter.
Steel	The minimum of the mass of steel in the lower plenum equipment and the mass limit specified via an input parameter

The amount and composition of the heavy metal layer generated through the reaction is evaluated based on a simplified quaternary phase diagram of U-Zr-O-Fe.[2] The results predicted by the model are compared against experimental data in Figure 2.
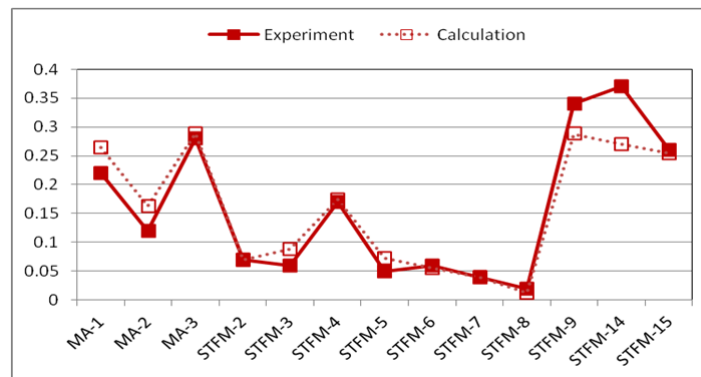

Figure 2, Comparison of heavy metal mass fraction between the model and MASCA experiment data.[2]

The corium structure is important because it determines the heat flux from the corium to the reactor vessel wall. The heat flux is non-uniform along the wall. The highest heat flux occurs at the section of the reactor vessel wall covered by the (upper) metal layer. It has been found that the thinner the metal layer is, the larger the heat flux to the wall. This is referred to as the "focusing effect." Under ideal conditions, there is a sufficient amount of metal to form a thick metal layer which reduces the focusing effect. However, if a heavy metal layer is formed, it may sequester some of the steel at the bottom of the corium pool, leaving a thinner top metal layer. In this condition, the focusing effect can be more pronounced.

The heat flux from the oxidic debris to the reactor vessel wall is driven by the convective heat transfer from the molten oxidic pool to the surrounding crust. The modeling approach in MAAP5.03 is to use empirical correlations for the convective heat transfer calculations. Currently there are three correlations available: the Jahn and Reineke correlation,[3] the BALI correlation,[4] and the ACOPO correlation.[5] These correlations provide not only the average convective heat transfer coefficients, but also the distribution of the heat transfer coefficient as a function of the inclination angle along the lower head wall. Figure 3 shows the comparison of the angular distribution used in MAAP5.03 and the experiment data.[3] The same correlations are also applied to the heat transfer from the heavy metal layer to the surrounding crust.
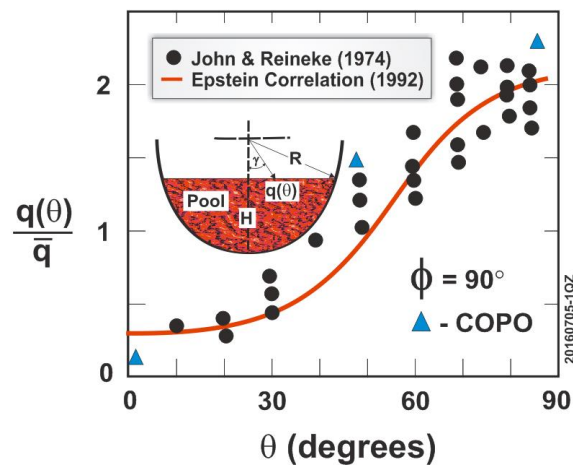
Figure 3, Comparison of the angular distribution used in MAAP5.03 and experiment data.[3]

One of the prime concerns in the analysis of IVR is heat transfer from the metal layer to the reactor vessel wall. Because there is no crust insulating the wall from the light metal layer, heat transfer from the top metal layer to the reactor vessel wall may result in a large enough heat flux to fail the vessel. In MAAP5.03, the axial direction heat transfer in the top metal layer is modeled with the Globe-Dropkin correlation,[6] while the lateral direction heat transfer modeled with the Churchill-Chu correlation.[7] In addition to these correlations, MAAP5.03 is equipped with a model to address eddy diffusivity when the light metal layer is very thin. The eddy diffusivity limits the heat flux because the lateral heat transfer relies on natural convection vortices. For a very thin metal layer, the scale of the vortices is small enough to impose additional heat transfer resistance which lowers the heat flux to the vessel wall. Figure 4 shows the comparison of the heat flux from the metal layer to the vessel wall with and without the eddy diffusivity model. If eddy diffusivity is considered, the heat flux to the reactor vessel wall will not increase as the thickness of the light metal layer approaches zero. Instead, it reaches a maximum and then decreases with decreasing thickness of the light metal layer.
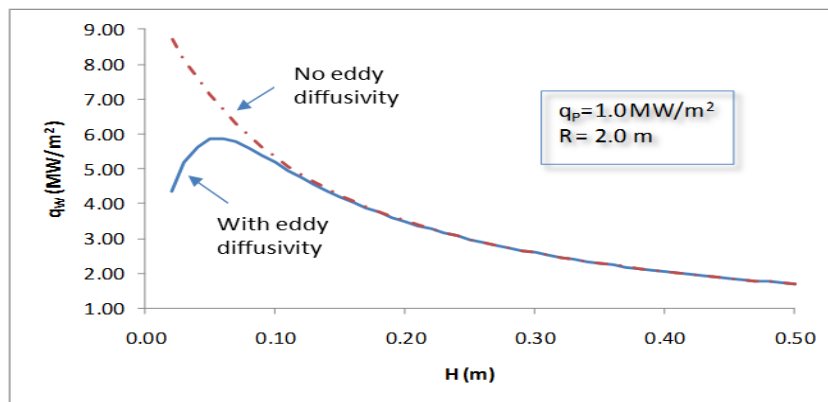

Figure 4, Comparison of heat flux from the light metal layer to the reactor vessel with and without the eddy diffusivity model.

III.B. REACTOR VESSEL FAILURE MECHANISMS

In MAAP5.03, five vessel failure mechanisms are considered for initial failure of a reactor vessel lower head:
1. Molten core debris attack on lower head penetrations may result in the melt entering the penetration channel. Once inside, the melt may refreeze and thereby plug the channel, or it could travel through the penetration line thereby increasing the wall temperature, heat and weaken the channel wall outside the vessel, potentially causing failure of the penetration.

2. Molten core debris attack and sustained heating from accumulated debris may lead to weakening of the penetration support weld and subsequent ejection of the penetration.
3. The combination of internal pressure and weight of the debris combined with high temperatures may result in creep rupture of the reactor vessel wall.
4. A coherent jet of debris impinging directly onto the lower head may cause localized ablation of the lower head.
5. A molten metal layer on top of the debris in the lower plenum may thermally attack and weaken the vessel wall.

Among the various vessel failure mechanisms, the failure of lower head penetrations (mechanism 1) was found to be the dominating failure mechanism for the PWR plant analyzed in this paper. It is worthwhile to discuss this mechanism in more detail. The first way a penetration tube failure can occur is due to corium intrusion into the penetration tube. The corium can be driven by the pressure difference between the reactor vessel and the containment to travel a significant distance in the tube before it is frozen. If the travel distance exceeds the length of the penetration tube from the vessel wall to the seal table, the penetration tube is considered to fail. Even if the travel distance is shorter than the length to the seal table, the penetration tube can also fail, if a) the heat transfer from the corium to the tube wall exceeds the limit that causes temperature to rise to the failure (softening) temperature; or b) the convective heat transfer from the outer surface of the penetration tubes to water or gas in the reactor cavity is less than the decay power of the solidified corium in the tube. The second way that penetration tube failure can occur is due to the failure of the penetration closure weld. If the weld fails, the tube can be ejected due to the pressure difference between the vessel and containment. MAAP5 evaluates the temperature at the closure weld, and the ultimate yield strength of the weld as the function of the temperature. If the penetration tube is fabricated from a different material than the reactor vessel wall, the thermal expansion of the penetration tube may provide additional support to balance the shear stress. However, if the shear stress exceeds the ultimate strength of the weld, the penetration tube is considered to fail because of tube ejection.

In typical MAAP runs, it is calculated that melting of the weld results in the ejection of the penetration tubes and the release of molten corium through the open penetration holes. However, two questions should be addressed regarding the MAAP calculation. First, is it possible that a corium crust covers the inside opening of the penetration hole that is strong enough to prevent the corium melt from entering the hole after the penetration tube is ejected? Secondly, even though the penetration tube is no longer attached to the vessel wall, is it possible that it remains in place in the penetration hole owing to external structural constraints to its motion? Both of these questions should be addressed for each plant outside of MAAP. Assuming that the penetration tube is fused to the guide tube, the penetration tube can not be forced out of the penetration hole unless the guide tube translates a distance equal to the thickness of the reactor vessel wall. The guide tube is constrained from moving by support plates through which the guide tube penetrates. Therefore, the penetration tube can be ejected from the penetration hole only if one of the guide tube segments between any two support plates (see Figure 5) fail by either bending stress buildup to the maximum tensile stress or by elastic instability. For plants with bottom penetrations and external vessel cooling, analysis addressing these two questions should be performed to determine whether penetration ejection can occur or not.
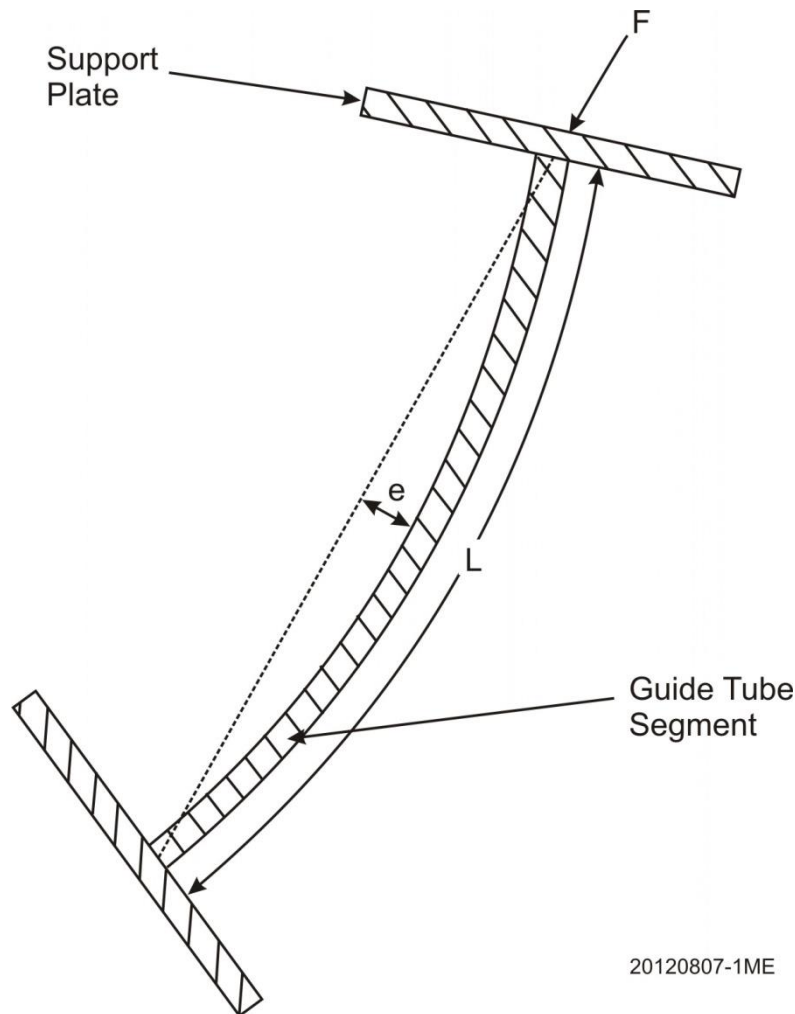
Figure 5, Guide tube segment between support plates, illustrating force loading, initial eccentricity e and length L.

This initial failure of the reactor vessel is treated as a localized failure, as opposed to an extensive rupture of the lower head. If a localized failure occurs on the side of the vessel, only the top debris layer above the failure location would be expelled, leaving behind most of the debris in the lower plenum. This implies that some of the debris can be retained in the vessel longer. The debris would still continue heating the lower plenum and may eventually lead to an extensive failure of the lower head, dumping all the debris into the containment. Hence, the size of the extensive failure is less important; it simply has to be large enough to cause a rapid expulsion of all debris from the lower plenum.

There are three conditions that lead to extensive failure of the lower head:
1. The localized failure occurs in the bottom node of the lower head due to creep rupture.
2. The localized failure occurs above the bottom node due to creep rupture and the damage fraction of the bottom node is greater than the user-supplied parameter FDAMLH.
3. After a localized failure, a creep rupture occurs in any lower head node (if the localized failure was due to creep rupture, the subsequent creep rupture must occur elsewhere).

After the reactor vessel is determined to be failed, MAAP calculates the radial ablation velocity of the failed area and the mass flow rate of ablating steel.

III.C. DEBRIS COOLING MECHANISMS

If water is present in the vessel, MAAP5.03 evaluates the heat transfer from the corium to the water. If a particle bed exists, the heat transfer from particle bed is calculated based on the Lipinski[8] or Henry[9] correlations. The heat transfer from the top of the metal layer to water is based on nucleate boiling and film boiling correlations. In addition to the heat transfer at

the top, MAAP5.03 also implements a gap cooling model. The gap cooling model accounts for a gap that may be created between the crust surrounding the oxidic debris and the reactor vessel wall. Water in the reactor vessel lower plenum may penetrate into the gap and cool the vessel wall from the inside. Heat removal by gap cooling is modeled with empirical correlations. There are three correlations available in MAAP5.03: the Monde correlation,[10] the Okano correlation,[11] and the Fauske correlation.[12] The Monde correlation is based on an experimental investigation of heated channels in a water pool. The Okano and Fauske correlations are based on counter-current experimental investigations of a heated gap in a water pool. The gap cooling model is active only when there is negligible amount of metal in the corium. Otherwise, the top metal layer is assumed to seal the gap and prevent water from penetrating into the gap.

One of the important severe accident mitigation strategies is to flood the reactor cavity so that the vessel can be cooled from the outside via ERVC. The critical heat flux (CHF) on the outer surface of the vessel wall imposes the thermal limit for the heat flux from the exterior surface of the reactor vessel wall to the surrounding pool of water. In designs such as AP1000 or APR1400, a baffle was added around the reactor vessel to create a cooling channel, so that natural circulation can be established between the water pool in the cavity and the cooling channel. The natural circulation flow increases the CHF and enhances the cooling of the reactor vessel wall. MAAP5.03 uses empirical correlations to model the heat transfer coefficient between the reactor vessel wall and the cooling channel. These include Yang's correlation[13] for a plain vessel with and without enhanced natural circulation for cooling channel designs similar to APR1400, and ULPU-2000 correlations for designs similar to AP1000.[5]

IV. ANALYSIS METHODOLOGY

The effectiveness of IVI and ERVC strategies for IVR are evaluated using MAAP5 code calculations. However, simply executing a single run cannot account for the uncertainties associated with the severe accident phenomena that are being modeled by the code. One approach to accounting for these uncertainties is to establish bounding assumptions. An example of this could be forcing early relocation of the entire core into the lower plenum in an effort to promote vessel failure. However, choosing bounding assumptions is not always straightforward for Level II analysis. For this example, concurrent relocation of the entire core can alter the heat transfer profile from the core debris in the lower plenum to the reactor vessel lower head wall. Specifically, this can result in a thicker light metal layer and reduced focusing effect. Thus, a poorly chosen bounding assumption can lead to a non-conservative result.

The method chosen to address uncertainty in this analysis is a Monte Carlo method. Instead of executing a single run with bounding assumptions, many runs are executed with sampled sets of parameters in order to cover the entire spectrum of plausible results. Each sample run includes randomly sampled values for approximately 80 input parameters. These input parameters were chosen to encapsulate the uncertainties in severe accident phenomena, modeling, and sequence initiator. The ranges and probability distributions of the sampled parameters were selected based upon comparisons of code calculations to experimental benchmark results.

The required number of completely random samples, N (the number of MAAP runs per base sequence), is given by what has been known as Wilks' formula.[14] The 2nd order Wilks' formula can be written as $1-a^N-N(1-a)a^{N-1} \geq b$ where $b \times 100$ is the confidence level (%) that the maximum code results will not be exceeded by the $a \times 100$ percentile of the corresponding output distribution.[15] The formula is satisfied with a=0.95 and b=0.95 when N=93. Therefore, if 93 randomly sampled MAAP runs are performed per base sequence there is a 95% confidence that the maximum code results exceed the 95th percentile of the distribution. The 95% confidence level and the 95th percentile value are reasonable criteria. In order to provide slightly more confidence, N=100 is adopted as the number of samples per sequence to be analyzed in this analysis. It should be noted that the 2nd order Wilks' formula is independent of the number of parameters included in the uncertainty analysis.

Thus, the steps in the method are:
1. Select the accident sequences to be analyzed and create input files to model the defined accident sequences.
2. Identify input parameters that potentially impact the results of interest and quantify the ranges and probability distributions of these parameters.
3. Create sets of samples for the selected input parameters and use the sample sets to generate input files.
4. Execute the generated input files using MAAP.
5. Process and analyze the results of the MAAP calculations to determine the probability of success.

In order to analyze the results, the key outputs must first be collected and tabulated. These tabulated results are then sorted into ascending order. Each result is then assigned a probability range. The size of each probability range is equal to one divided by the number of runs (N). A cumulative distribution function (CDF) is constructed by plotting each result value (R_i) as spanning from probability $(i-1)/N$ to i/N where i represents the result rank in the ordered result list. A diagram of this process is shown in Figure 6. This process allows for investigation into the calculated values that drive the result.
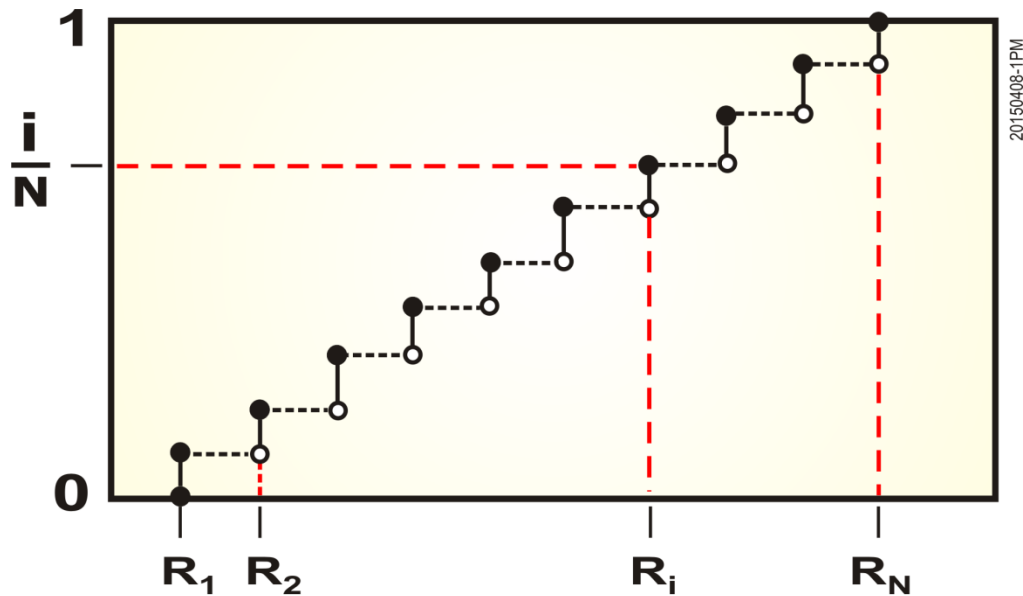
Figure 6, Process of creating a CDF from sorted run results.

One hundred sample runs were executed using the MAAP5.03 code for each operator action delay time for each defined accident sequence. This yielded thousands of MAAP results which were analyzed to determine whether or not vessel failure occurred in each. The probability of vessel failure was then determined as the number of samples with vessel failure divided by the total number of samples.

V. RESULTS AND DISCUSSION

Sample results of analyzing the probability of vessel failure using the MAAP5.03 code are shown in Figure 7 and Figure 8. Figure 7 shows the probability of vessel failure for a small LOCA occurring at full power. The plot shows that, for this example, ERVC alone is not sufficient to save the vessel for a severe accident initiated at full power. When using only ERVC as a mitigating strategy, the lowest calculated probability of vessel failure is approximately 67%. The dominant vessel failure mode is ejection of the instrument tubes. The instrument tube ejection mode of vessel failure contributes a 67% chance of vessel failure for all analyzed mitigation action delay times. The remaining occurrences of vessel failure are nearly all due to creep rupture.

IVI is more effective than ERVC for the small LOCA occurring at full power. Prompt implementation of IVI can cool the core while it is still within the core boundary. This is the most probable way to maintain vessel integrity. The results show that the probability of failing the vessel increases in a manner roughly proportional the amount of debris that relocates to the lower plenum. This reflects the fact that gap cooling becomes increasingly ineffective with increasing melt pool depth because the water is unable to penetrate to the lower portions of the reactor vessel lower head prior to being converted into steam. The result of the calculation shows that the vessel failure mode is approximately evenly split between instrument tube ejection and creep rupture. The simultaneous implementation of IVI and ERVC provides only a marginal benefit over using IVI alone.

Figure 8 shows the probability of vessel failure for a loss of shutdown cooling occurring during mid-loop operation (POS 5). This plot shows that using ERVC as a mitigation strategy is much more likely to succeed at reduced decay power levels. The decay power associated with an accident occurring at POS 5 is approximately half of that associated with the small LOCA occurring at full power. The lower decay power allows the inside surface of the vessel wall to stay at a lower temperature. This can prevent failure of the instrument tube penetration closure welds when ERVC is implemented early enough.

IVI is more effective than ERVC when implemented promptly for a loss of shutdown cooling during POS 5. However, as the mitigation action delay time increases, ERVC is calculated to be slightly more effective than IVI.
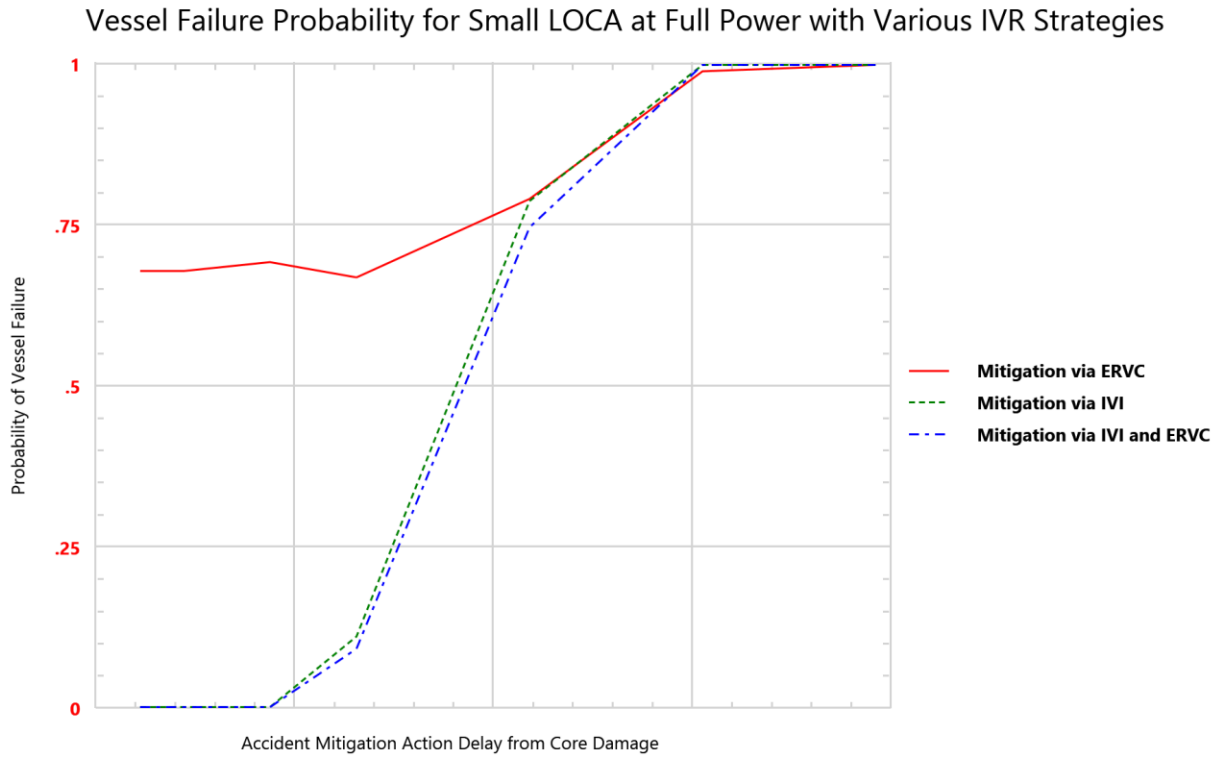
Figure 7, Analysis results for vessel failure probability for initiators occurring at full power.
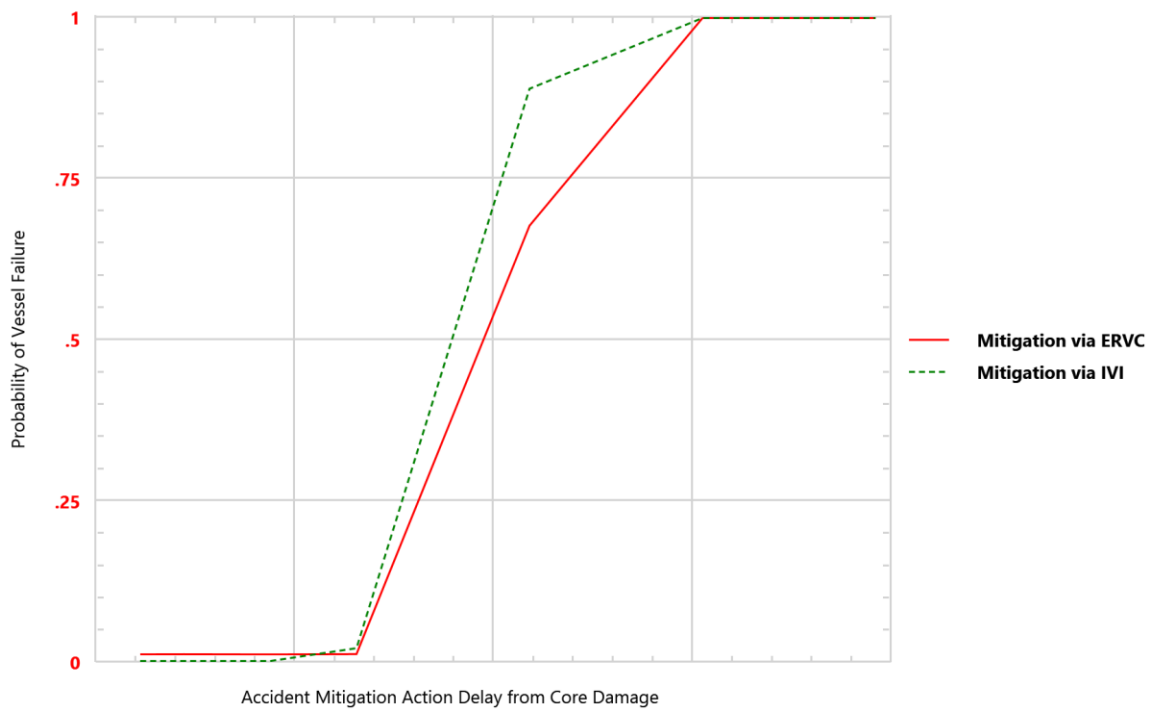

Figure 8, Analysis results for vessel failure probability for initiators occurring at shutdown conditions.

The probability of vessel failure due to each of the vessel failure mechanisms is shown in Figure 9 for an initiator occurring at full power that is mitigated by ERVC only. The dominant vessel failure mechanism is failure by means of instrument penetration tube ejection. The figure shows that this vessel failure mechanism is dominant regardless of the delay in implementing ERVC. However, as ERVC actuation is further delayed, the probability of vessel failure due to creep rupture increases. Figure 10 shows the time history of heat flux ratio for a sequence with successful IVR due to implementation of ERVC as a mitigating strategy. The heat flux ratio plotted in this figure is the ratio of the nucleate boiling heat flux on the outside surface of the reactor vessel to the critical heat flux on the outside surface of the reactor vessel. The critical heat flux in this example is calculated based upon an enhanced insulation design to promote ex-vessel cooling. The heat flux ratio becomes non-zero after the first relocation of core material into the lower plenum. When this occurs, the heat flux ratio on the outside surface of the reactor vessel wall is calculated to be approximately 25%. After the debris in the reactor vessel lower head heats up and achieves its end state configuration (see Figure 1), there is significant ablation of the vessel wall section that is in contact with the light metal layer. The ablation causes the wall to thin until the heat transfer on the outside surface matches the heat transfer from the light metal layer. This coincides with a sharp rise in the temperature on the outside surface of the reactor vessel wall which increases the nucleate boiling heat flux and the heat flux ratio. As shown in the figure, the heat flux ratio levels off near 83% and begins to decrease. For this sample sequence, IVR is successful due to the timely implementation of ERVC.
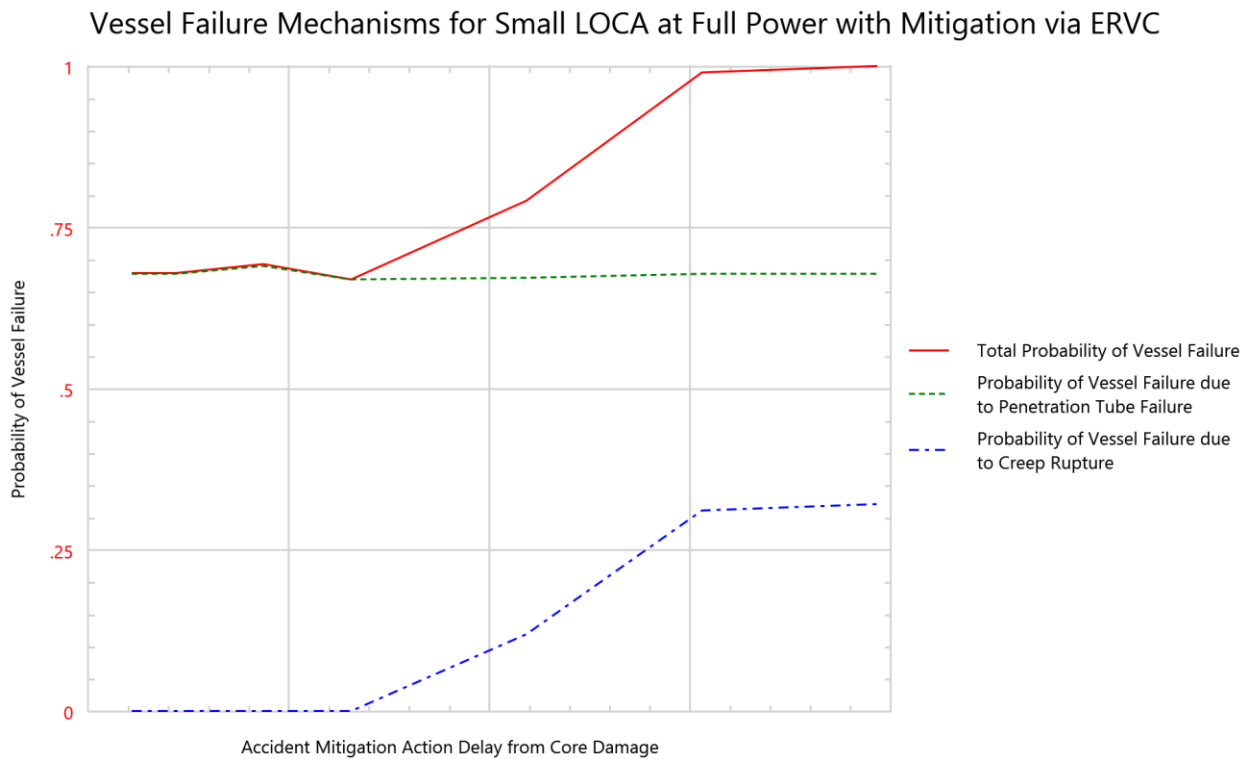

Figure 9, Vessel failure mechanism probabilities for initiators occurring at full power with mitigation via ERVC.
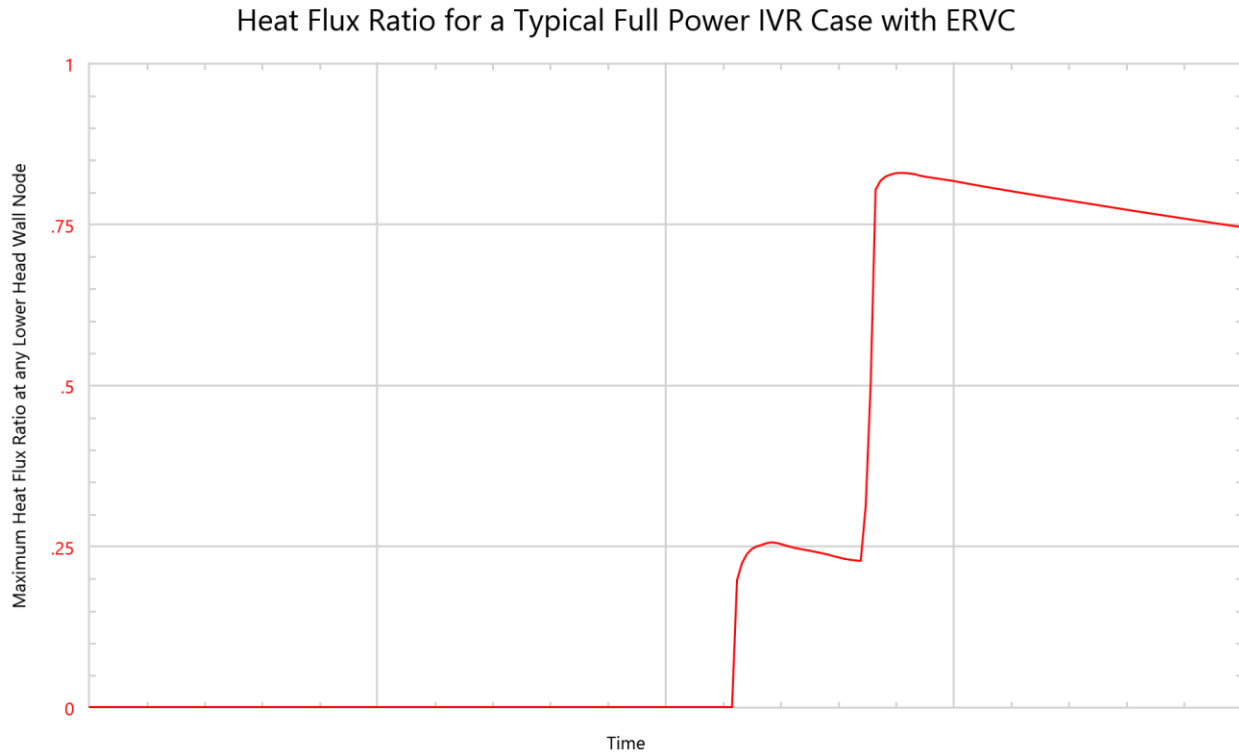
Figure 10, Time history of a typical heat flux ratio for a full power initiator with successful IVR via ERVC.

VI. SUMMARY

A method has been described for the application of the MAAP5 computer code to the analysis of severe accident management strategies for the prevention of vessel failure. The method calculates the probability of vessel failure as a function of the mitigation action delay time. Sample calculations were performed for initiators occurring at both full power and during shutdown conditions. These sample calculations show that MAAP is an efficient tool to use for the analysis of severe accident mitigation strategies. The effectiveness of IVR as a severe accident mitigation strategy is dependent on several plant-specific factors: decay power level, the presence of penetrations in the reactor vessel lower head, the reactor vessel insulation design, and the capability to reliably depressurize the reactor vessel.

REFERENCES

1. Electric Power Research Institute, *MAAP5 Modular Accident Analysis Program for LWR Power Plants, Transmittal Document for MAAP5 Code Revision MAAP5.03*, EPRI, August, 2015.
2. Salay, M., Fichot, F., *Modelling of Corium Stratification in the Lower Plenum of a Reactor Vessel*, OECD/NEA MASCA Seminar, Aix-en-Provence, France, June 10th to 11th, 2004.
3. Jahn, M., and Reineke, H. H., *Free Convection Heat Transfer With Internal Heat Sources, Calculations and Measurements*, Proc. of the 5th Intl. Heat Transfer Conf., Tokyo, Japan, Paper NC2.8, 1974.
4. Bonnet, J. M., and Seiler, J. M., *Thermal-Hydraulic Phenomena in Corium Pools for Ex-Vessel Situations: the BALI Experiment*, Proceedings of the International Conference on Nuclear Engineering (ICONE 7), Tokyo, Japan, April 19-23, 1999.
5. Theofanous, T. G., Liu, C., Additon, S., Angelini, S., Kymalainen, O., Salmassi, T., *In-Vessel Coolability and Retention of a Core Melt*, DOE/ID-10460, October 1996.
6. Globe, S., and Dropkin, D., *Natural Convection Heat Transfer in Liquids Confined by Two Horizontal Plates and Heated From Below*, ASME Journal of Heat Transfer, Vol. 81, p. 24, 1959.
7. Churchill, S., and Chu, H., *Correlating Equations for Laminar and Turbulent Free Convection from a Vertical Plate*, International Journal of Heat and Mass Transfer, 1323-1329, 1975.

8. Lipinski, R. J., *A Particle-Bed Dryout Model with Upward and Downward Boiling*, Trans. Am. Nucl. Soc. 35, pp. 358-360, 1980.

9. Henry, R. E., Epstein, M., Fauske, H. K., *Cooling of Debris Beds—Methods of Analyses for LWR Safety Assessments*, Proceedings of the International Meeting on Thermal Nuclear Reactor Safety, NUREG/CP-0027, Chicago, pp.1421~1432, Aug. 29~Sep. 2, 1982.

10. Monde, M., Kusuda, H., and Uehara, H., *Critical Heat Flux During Natural Convective Boiling in Vertical Rectangular Channels Submerged in Saturated Liquid*, ASME Journal of Heat Transfer, Vol. 104, pp. 300-303 May 1982.

11. Okano, Y., Nagae, T., Murase, M., *Modeling and validation of in-vessel debris cooling during LWR severe accident*, J. Nucl. Sci. Tech., 42, pp. 351-361, 2005.

12. Fauske, H. K., *Operation of Reflux Condensation and Flooding Limitations*, FAI Process Safety News, Volume 9, Number 1, Spring 2002.

13. Yang, J., Cheung, F. B., Rempe, J. L., Suh, K. Y., and Kim, S. B., *Correlation of Nucleate Boiling Heat Transfer and Critical Heat Flux for External Reactor Vessel Cooling*, 2005 ASME Summer Heat Transfer Conference, San Francisco, CA, 17-22, July 2005.

14. Wilks, S. S., *Statistical Prediction with Special Reference to the Problem of Tolerance Limits*, The Annals of Mathematical Statistics, Volume 13, Number 4, 1942.

15. Glaeser, H., *GRS Method for Uncertainty and Sensitivity Evaluation of Code Results and Applications*, Science and Technology of Nuclear Installations, Vol. 2008, Article ID 798901, Hindawi Publishing Corporation, 2008.